Cancer Research

Mast Cell Targeting Hampers Prostate Adenocarcinoma Development but Promotes the Occurrence of Highly Malignant Neuroendocrine Cancers

Paola Pittoni[1], Claudio Tripodo[2], Silvia Piconese[1], Giorgio Mauri[1], Mariella Parenza[1], Alice Rigoni[1], Sabina Sangaletti[1], and Mario P. Colombo[1]

Abstract

Mast cells (MC) are c-Kit–expressing cells, best known for their primary involvement in allergic reactions, but recently reappraised as important players in either cancer promotion or inhibition. Here, we assessed the role of MCs in prostate tumor development. In prostate tumors from both tumor-prone transgenic adenocarcinoma of the mouse prostate (TRAMP) mice and human patients, MCs are specifically enriched and degranulated in areas of well-differentiated (WD) adenocarcinoma but not around poorly differentiated (PD) foci that coexist in the same tumors. We derived novel TRAMP tumor cell lines, representative of WD and PD variants, and through pharmacologic stabilization or genetic ablation of MCs in recipients mice, we showed that MCs promote WD adenocarcinoma growth but are dispensable for PD tumors. WD tumors rely on MCs for matrix metalloprotease 9 (MMP-9) provision, as reconstitution of MC-deficient mice with wild-type but not MMP-9$^{-/-}$ MCs was sufficient to promote their growth. In contrast, PD tumors are MMP-9 self-competent, consistently with epithelial-to-mesenchymal transition. Such a dual source of MMP-9 was confirmed in human tumors, suggesting that MCs could be a good target for early-stage prostate cancer. Interestingly, in testing whether MC targeting could block or delay tumorigenesis in tumor-prone TRAMP mice, we observed a high incidence of early and aggressive tumors, characterized by a neuroendocrine (NE) signature and c-Kit expression. Taken together, these data underscore the contribution of MCs in tumor progression and uncover a new, opposite role of MCs in protecting against the occurrence of aggressive NE variants in prostate cancer. *Cancer Res; 71(18); 5987–97.* ©*2011 AACR.*

Introduction

In Western countries, prostate cancer accounts for the second most frequent cause of death from cancer in men (1). Prostatic carcinoma is often a multifocal disease, in which multiple histologic patterns, reflective of the varied differentiated aptitude of the neoplastic clone, may coexist within a single tumor (2). Such a spectrum of histologic lesions includes well-differentiated (WD) adenocarcinomas as well as poorly differentiated (PD) or undifferentiated cancers. Patients are classified and treated according to disease extension: those with organ-confined cancer undergo radical prostatectomy or radiotherapy, whereas those with metastatic or recurrent disease are subject to hormone therapy aimed at androgen deprivation of malignant cells. Nonetheless, 18 to 36 months after an initial response to anti-androgen therapy, most prostate carcinomas switch to a hormone-resistant phenotype, entering into a more aggressive and ultimately fatal stage of disease. Foci of neuroendocrine (NE) cells are seen in virtually all cases of prostatic carcinoma; however, an extensive NE differentiation is associated with androgen independence, refractoriness to treatment, and poor prognosis (3).

The same heterogeneous histologic features of human prostate cancer can be found in tumors from mouse counterparts, such as the transgenic adenocarcinoma of the mouse prostate (TRAMP), in which SV40 large T antigen oncogene expression, driven by the rat probasin promoter, induces prostate transformation (4, 5). As in men, prostate cancers of TRAMP mice may switch, upon castration, from slowly growing adenocarcinoma to aggressive PD tumors with an NE phenotype (6).

Mast cells (MC) are granulocytic immune cells best known for their role in allergy and anaphylaxis, with important functions in innate immunity against bacteria, viruses, and

Authors' Affiliations: [1]Molecular Immunology Unit, Department of Experimental Oncology and Molecular Medicine, Fondazione IRCCS "Istituto Nazionale dei Tumori", Milan; and [2]Department of Human Pathology, University of Palermo, Palermo, Italy

Note: Supplementary data for this article are available at Cancer Research Online (http://cancerres.aacrjournals.org/).

Current address for S. Piconese: Dipartimento di Medicina Interna e Specialità Mediche, Sapienza University, Policlinico Umberto I, Rome, Italy.

Corresponding Author: Mario P. Colombo, Fondazione IRCCS Istituto Nazionale dei Tumori, via Amadeo 42, 20133 Milan, Italy. Phone: 39-022-390-2252; Fax: 39-022-390-2630; E-mail: mario.colombo@istitutotumori.mi.it

doi: 10.1158/0008-5472.CAN-11-1637

parasites. Since their first description in the late 19th century, MCs were found aggregated around and within many types of solid cancers, but only in recent years the multiple functions operated by MCs in fostering angiogenesis, tissue remodeling, and immunomodulation in human and murine cancer have emerged. MCs may exert pro- or antitumoral roles, depending on tumor type, on microenvironmental signals and on neighboring interacting cells (7). Such functional complexity may explain the discrepancy emerging from different studies, showing opposite correlations of MC accumulation with prognosis in different settings (8). In this scenario, prostate cancer is no exception; several studies on human prostate tumor samples have tried to address this issue (9–13), but no conclusive data exist about the actual role of MCs in promoting or suppressing cancer at this site. In a recent work, peritumoral MCs were shown to enhance angiogenesis and tumor growth in the orthotopic AT-1 rat prostate tumor model and MCs were seen recruited in the peritumoral compartment in men during the formation of androgen-independent prostate cancer (14), recommending MCs as a novel target for prostate tumor therapy. However, in the same study, high MC numbers in the intratumoral compartment were shown to be associated with a favorable outcome in patients, implying that the actual role of MCs in prostate cancer is indeed context dependent and that MC targeting has to be carefully evaluated before being introduced into the clinic.

Here, we analyze the role of MCs in transgenic mouse prostate tumors and show that MCs exert different functions according to the tumor subtype. We confirm that MCs are essential players in the initial stages of prostate tumor progression, by supplying matrix metalloprotease 9 (MMP-9) in the microenvironment, but become dispensable at post–epithelial-to-mesenchymal transition (EMT) stages. These data are mirrored by MC distribution and MMP-9 expression in tumor foci from human prostate biopsies. Moreover, we provide the first evidence that MC inactivation may end up with the paradoxical occurrence of fatal NE tumor variants, an observation that must be taken into account before proposing MC-targeted antitumor therapies.

Materials and Methods

Mice, tumor cell lines, and treatments

C57BL/6 mice were purchased from Charles River. c-Kit mutant *C57BL/6-Kit$^{W\text{-}sh/W\text{-}sh}$* (*Kit$^{W\text{-}sh}$*) mice were purchased from Jackson Laboratories and intercrossed twice to C57BL/6, to obtain congenic C57BL/6-Kit$^{+/+}$ littermates to be used as controls. TRAMP mice on C57BL/6 background were kindly provided by Dr. Vincenzo Bronte (IRCCS Istituto Oncologico Veneto, Padova, Italy), under agreement with Dr. Norman Michael Greenberg (Fred Hutchinson Cancer Research Center, Seattle, WA). MMP-9$^{+/-}$ mice on C57BL/6 background were kindly provided by Dr. Leif Lund (Panum Institute, Department of Experimental Medicine, University of Copenhagen, Copenhagen, Denmark) and intercrossed to obtain homozygous MMP-9$^{-/-}$ mice. Mice were maintained under pathogen-free conditions at the animal facility of Fondazione IRCCS "Istituto Nazionale dei Tumori." Animal experiments were authorized by the Institute Ethical Committee and carried out in accordance to institutional guidelines and national law (DL116/92).

Prostate tumor cell lines were obtained in our laboratory from heterogeneous 28 to 32 weeks old prostatic adenocarcinomas from male TRAMP mice (as described in ref. 15). Multiple lines were established on the basis of different growth rates and cell morphology.

Wild-type and *Kit$^{W\text{-}sh}$* mice were injected with prostate tumor cell lines (2×10^6 cells) subcutaneously in the flank, and tumor growth was measured with a caliper once a week and recorded as longest diameter $\times$ (shortest diameter)^2 (in cubic millimeters). In the orthotopic setting, 2×10^6 tumor cells were inoculated in the prostate anterior lobe of wild-type and *Kit$^{W\text{-}sh}$* mice. The growth of orthotopically injected tumor lines and of spontaneous tumors in TRAMP mice was echographically monitored using a Vevo 770 micro-ultrasound imaging system (Visualsonics Inc.), as described (16). The invasive capacity of prostate lines was evaluated using the Cell Invasion Assay Kit (Chemicon International) according to manufacturer's instruction. Sodium cromoglycate (cromolyn; Sigma-Aldrich) was intraperitoneally (i.p.) injected in mice daily (10 mg/kg, dissolved in saline), starting 1 or 5 days after tumor cell line injection (as indicated for each experiment), or at 6 to 8 weeks of age in TRAMP mice, and continuing for the duration of the experiment.

Histology, immunohistochemistry, and flow cytometry

Histopathologic and immunohistochemical analyses were carried out on formalin-fixed and paraffin-embedded specimens. MC distribution and density on mouse tissues were estimated by staining slides with toluidine blue as previously reported (17); MCs were counted out of 5 high-power microscopic fields (400×), and counts were expressed as average.

Immunohistochemistry and flow cytometry were carried out as detailed in the Supplementary Material.

Human prostate cancer samples were gathered from the archives of the Human Pathology Section of the University of Palermo School of Medicine. Archival samples representative of the whole spectrum of preneoplastic and neoplastic alterations, namely glandular epithelial hyperplasia ($n = 5$), prostatic intraepithelial neoplasia (PIN)/*in situ* adenocarcinoma ($n = 5$), WD/moderately differentiated infiltrating adenocarcinoma (Gleason score 1–3; $n = 5$), and PD/undifferentiated carcinomas (Gleason score 4–5; $n = 6$), were selected. MC counts on human samples were carried out on sections immunostained using an anti-human tryptase monoclonal antibody (clone 10D11; Novocastra). The number of tryptase-positive cells was counted out of 5 high-power microscopic fields, and counts were expressed as average. All slides were analyzed under a DM2000 optical microscope (Leica Microsystems), and microphotographs were collected using a DFC320 digital camera (Leica).

Stem cell factor, VEGF, and MMP-9 detection

Stem cell factor (SCF), VEGF, and MMP-9 were measured in cell culture supernatants, mouse sera, or tumor tissue cultures

by sandwich ELISA using the DuoSet ELISA Development System for mouse SCF (R&D Systems), the Murine VEGF Development Kit (Peprotech, Inc.), and the Quantikine Total MMP-9 ELISA Kit (R&D System), respectively, according to manufacturer's instruction. Sera from mice were collected as previously described (18).

Bone marrow–derived MC differentiation and reconstitution of *Kit*$^{W\text{-}sh}$ mice

Bone marrow–derived MCs (BMMC) were obtained by *in vitro* differentiation of bone marrow cells taken from mouse femurs and tibias, in the presence of interleukin 3 and SCF (20 ng/mL each; Peprotech), as described (19). After 5 weeks of culture, BMMCs were monitored for FcεRI and c-Kit expression by flow cytometry, and purity was more than 90%. BMMCs were obtained from pools of 3 to 4 mice in each experiment. For MC reconstitution studies, BMMCs derived from wild-type or MMP-9$^{-/-}$ mice were transferred by intradermal injection into 8 weeks old *Kit*$^{W\text{-}sh}$ male mice (5×10^6 cells in 4×50 μL aliquots in PBS in a row down the length of shaved left flank skin). Tumor cell lines were injected 6 to 8 weeks after adoptive transfer of BMMCs.

Gene expression profiling

RNA was isolated from prostate cell lines, prostates from 30 weeks old C57BL/6 mice, and spontaneous tumors from 30 weeks old TRAMP mice, 24 weeks old *Kit*$^{W\text{-}sh}$TRAMP mice, and 24 weeks old cromolyn-treated TRAMP mice, using the guanidinium thiocyanate/cesium chloride gradient method (20). mRNA expression profiles were analyzed on an Illumina microarray platform as detailed in Supplementary Data. All array data have been deposited in National Center for Biotechnology Information's Gene Expression Omnibus (GEO) and are accessible through GEO series accession number GSE29958. Class comparison analysis to identify differentially expressed genes between different tumor cell lines, or between different TRAMP tumors, was carried out using the GenePattern Software (Broad Institute-MIT; ref. 21). The program ran a paired *t* test using the random variance model, and differences of expression with a value of $P < 0.05$ were considered significant.

Statistical analysis

Results are expressed as the means ± SD, unless differently indicated. Comparisons between 2 groups were carried out with the 2-tailed Student *t* test for unpaired samples, applying correction for unequal variances when required. Tumor-take curves were compared with the Mann–Whitney *U* test (2-tailed). In all tests, the value of $P < 0.05$ was considered significant.

Results

MCs are enriched and degranulated in areas of WD adenocarcinoma but not in PD lesions in TRAMP tumors

To evaluate MC infiltration in prostates from TRAMP mice, we assessed the frequency of c-Kit$^+$ FcεRI$^+$ cells among prostatic CD45$^+$CD11b$^-$ cells by flow cytometric analysis at 16 to 18, 22 to 24, and 30 to 32 weeks of age. Very few c-Kit$^+$ FcεRI$^+$ cells could be detected in prostates from young TRAMP mice, but their frequency increased up to 9% of CD45$^+$ cells in tumoral prostates from 30 to 32 weeks old TRAMP mice and was significantly higher than that found in age-matched wild-type prostates (Fig. 1A and B).

Toluidine blue staining of TRAMP prostates allows the visualization of MCs in tumor areas and peritumoral tissue at different stages of progression (Fig. 1D), classified according to the Bar Harbor consensus report of prostate lesions in genetically engineered mice (22). Prostate glands with signs of slight epithelial hyperplasia did not show accumulation of MCs in the stroma. However, an increased number of MCs were observed at sites of atypical epithelial hyperplasia/PIN. Such an increase became more conspicuous in areas of adenocarcinoma, where clustered MCs showed signs of degranulation. Strikingly, MC number dropped dramatically in PD/anaplastic foci (Fig. 1C and D).

These data show that MCs infiltrate spontaneous prostate tumors and significantly increase in number upon tumor progression from PIN to WD adenocarcinoma but are absent around foci of PD/anaplastic adenocarcinoma.

Novel TRAMP tumor cell lines phenocopy WD and PD prostate tumors also in terms of MC infiltration

To further analyze the functional role of MCs in prostate tumors in relation to different histologic patterns, we derived and characterized a set of novel tumor cell lines from prostates of 28 and 32 weeks old TRAMP mice. These novel cell lines were reflective of at least 2 distinct stages of tumor progression, displaying *in vitro* either a distinctive epithelial morphology (Fig. 2A, top inset) or a round-to-spindle morphology (Fig. 2A, bottom inset). Two of these novel cell lines, T1525 and T23, were selected as representative models of WD and PD/anaplastic prostate tumors, respectively (Supplementary Fig. S1), and used in further experiments. All results were then confirmed with at least one additional cell line per tumor type (data not shown). Both cell lines were tumorigenic when injected subcutaneously or orthotopically in adult C57BL/6 male mice. T1525, which maintained an epithelial morphology, gave rise to adenocarcinomas characterized by a pseudoglandular structure, whereas T23, reflective of EMT, originated tumor nodules mirroring PD/anaplastic TRAMP cancers in terms of morphology (Fig. 2A).

MC infiltration in these tumors recapitulated our observations on spontaneous TRAMP prostate tumors; accordingly, toluidine blue staining identified MCs infiltrating WD, but not PD tumors (Fig. 2B and C). This was not due to a generic lack of bystander infiltrating cells in PD nodules, because staining with anti-CD3 showed no significant difference in T-cell infiltrate between WD and PD tumors (Supplementary Fig. S2). Notably, WD T1525, but not PD T23 cell line, was found to produce the c-Kit ligand SCF, in both membrane-bound and secreted form (Supplementary Fig. S3A and B). In addition, SCF was detected in the sera of T1525, but not T23, tumor-bearing mice at concentrations directly correlating with tumor volume (Supplementary Fig. S3C).

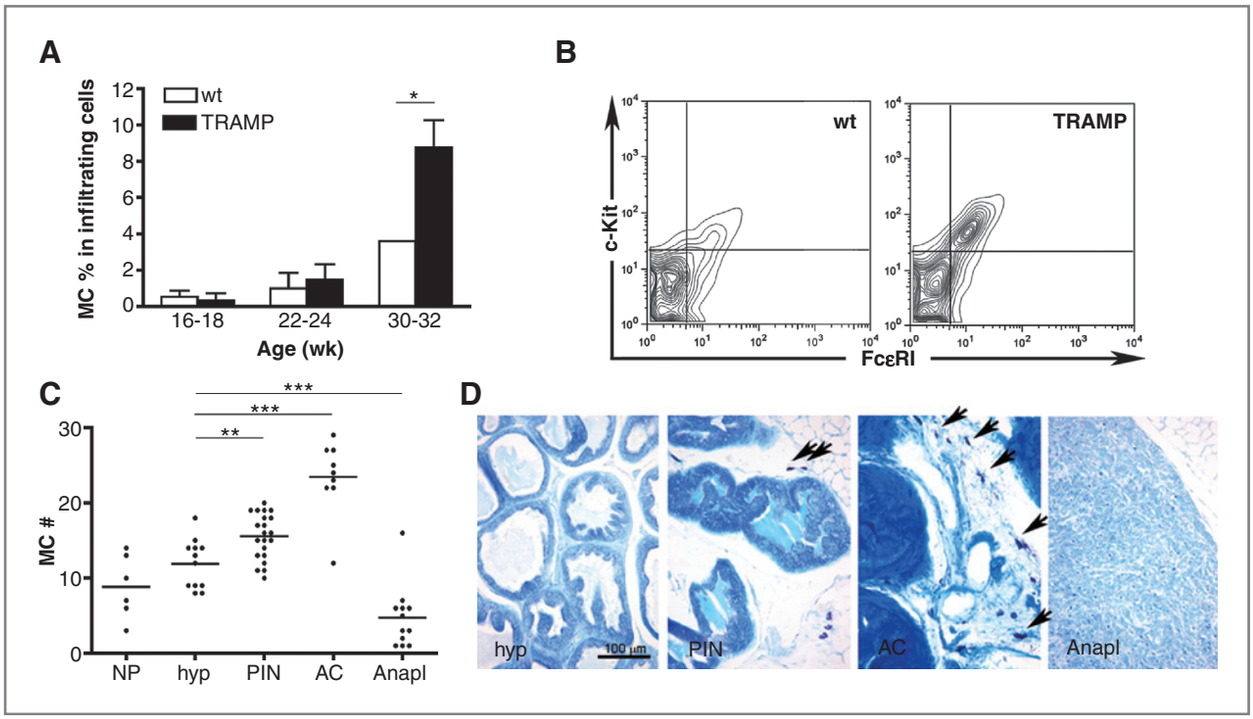

Figure 1. MCs are enriched and degranulated in areas of WD adenocarcinoma, but not in PD lesions, in TRAMP tumors. A, mean percentages of MCs infiltrating prostates from TRAMP mice and nontransgenic controls [wild-type (wt)] at different ages (3 mice/group). MCs were identified by flow cytometry as $CD45^+CD11b^-$ c-Kit^+ $Fc\varepsilon RI^+$ cells. B, representative plots of prostate-infiltrating MCs in wt and TRAMP mice at 30 to 32 weeks of age. C, MC counts carried out on toluidine blue–stained prostate sections from TRAMP mice of different ages, characterized by normal prostatic epithelium (NP), epithelial hyperplasia (hyp), PIN, overt adenocarcinoma (AC), and anaplastic foci (anapl). Three to 7 samples per histologic type were analyzed. D, toluidine blue staining of representative samples from TRAMP mice as in (C). Arrows indicate MCs. *, $P < 0.05$; **, $P < 0.01$; ***, $P < 0.005$.

Taken together, these data show a strong association between high MC infiltrate and prostate adenocarcinomas, likely because of their SCF secretion. Such an association is not found in PD cancers, which have undergone EMT.

MCs are both necessary and sufficient for WD prostate tumor growth

Two different mouse models of spontaneous/inducible carcinogenesis, affecting areas other than the prostate, showed infiltration of MCs in early lesions (23, 24). In both models, MCs played a causative role in tumor development by releasing inflammatory molecules promoting neoangiogenesis and tumor invasiveness. To verify whether MCs have a protumorigenic role in the early phases of prostate carcinogenesis, we blocked MC function by using both pharmacologic and genetic approaches. Sodium cromoglycate (cromolyn) inhibits MC degranulation and release of inflammogens (25). We injected the WD line T1525 subcutaneously in male wild-type mice and, when tumors were palpable, we treated mice daily with cromolyn for 3 weeks, a treatment that significantly inhibited tumor growth (Fig. 3A). If the treatment began the same day of tumor injection, it completely prevented tumor onset in most mice (data not shown). Cromolyn did not show a direct inhibitory effect on T1525 tumor growth *in vitro* (data not shown).

To validate independently the essential contribution of MCs in prostate tumorigenesis, we took advantage of MC-deficient $Kit^{W\text{-}sh}$ mutant mice. These mice carry a genetic inversion in the *Kit* gene promoter, which breaks a positive element controlling c-Kit expression specifically in MCs, and exhibit therefore profound MC deficiency in multiple organs, including dermis and prostate (26). In line with results obtained with cromolyn treatment, the WD line T1525 failed to grow in 90% of $Kit^{W\text{-}sh}$ mutant mice when injected either subcutaneously (Fig. 3B) or orthotopically (Fig. 3D and E). To rule out that cells other than MCs, which may be affected by the $Kit^{W\text{-}sh}$ mutation (27), might contribute to cancer outgrowth, we generated an MC knock-in system by locally reconstituting $Kit^{W\text{-}sh}$ mice with wild-type BMMCs and assessing MC ability to restore tumor growth. A total of 5×10^6 BMMCs were intradermally injected in the left flank of $Kit^{W\text{-}sh}$ mice. Two months later, reconstituted mice were injected in the same flank with T1525 tumor cells. In these mice, tumors did develop with an incidence and kinetics similar to wild-type controls, whereas no tumors developed in the majority of non-reconstituted $Kit^{W\text{-}sh}$ mice (Fig. 4D). Consistently with the positive outcome of MC injection, tumors from reconstituted mice were richly infiltrated by MCs (Supplementary. Fig. S4).

Of note, PD tumor line T23 grew in $Kit^{W\text{-}sh}$ mice as well as in wild-type controls (Fig. 3C), indicating its independence from MCs for growth.

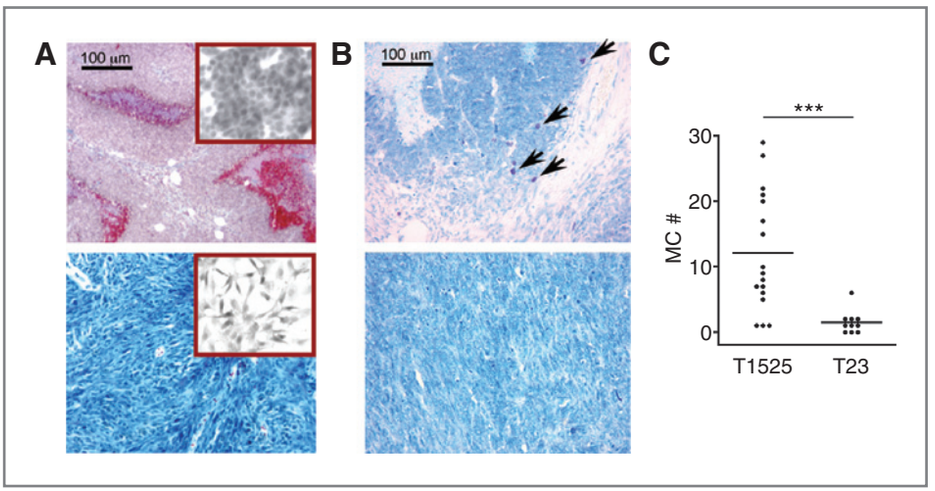

Figure 2. Novel TRAMP tumor cell lines phenocopying WD and PD prostate tumors are differentially infiltrated by MCs. A, representative Masson's trichrome and (B) toluidine blue staining of tumors originated by subcutaneous injection of T1525 (top) and T23 (bottom) cells in wild-type mice. Insets in (A) show hematoxylin and eosin staining of T1525 (top) and T23 (bottom) cell cultures *in vitro*. Arrows indicate infiltrating MCs. C, MC counts carried out on toluidine blue–stained sections from 3 T1525 and 3 T23 tumors. ***, $P < 0.005$.

Taken together, these data show that MCs are both necessary and sufficient for the growth of WD but dispensable for PD prostate tumors.

MCs favor the growth of WD adenocarcinoma through MMP-9 production

According to a model proposed on epithelial carcinogenesis (23), we hypothesized that WD, but not PD, prostate tumors might depend on MCs for provision of factors favoring angiogenesis and tumor invasiveness. Indeed, MCs are a source of VEGF, basic fibroblast growth factor, and TNF-α (28). They also produce MMP-9 (ref. 29; Supplementary Fig. S5A), a matrix-degrading enzyme-promoting tumor invasiveness. MMP-9 is also crucially involved in the mobilization of bioactive VEGF from the extracellular matrix (ECM; ref. 18), helping the switch from vascular quiescence

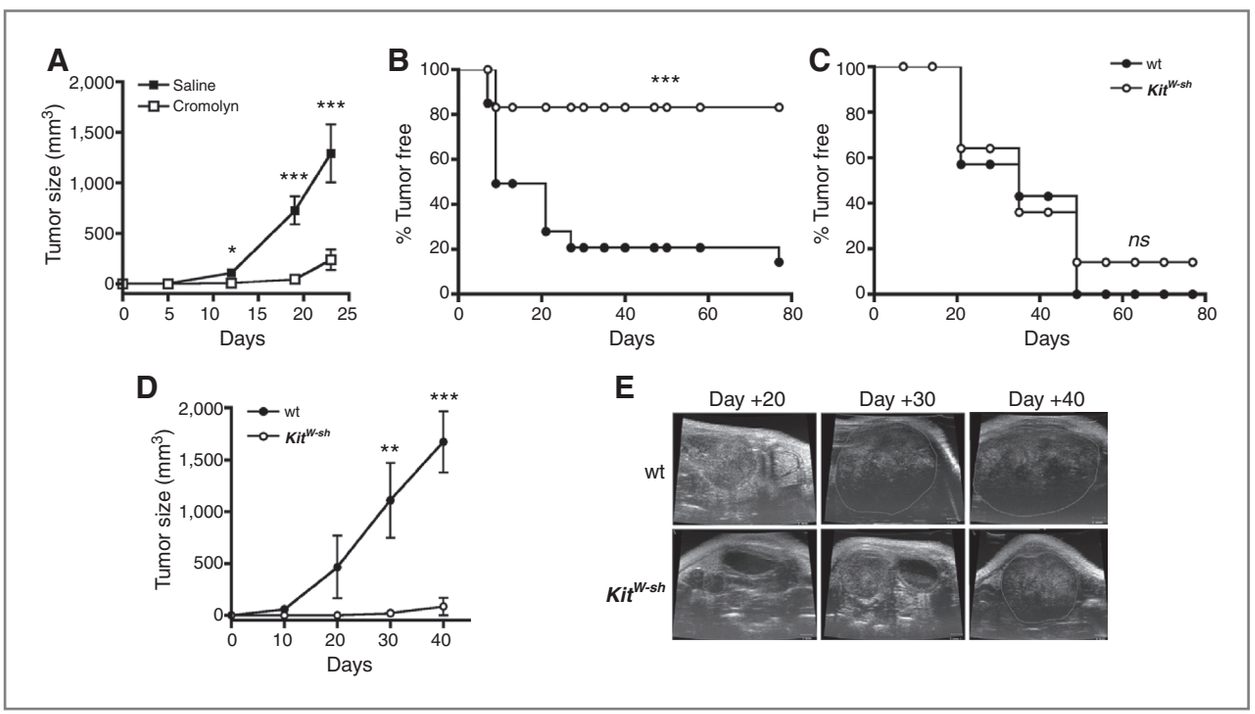

Figure 3. MCs are both necessary and sufficient to promote WD prostate tumor growth. A, tumor size (± SEM) in wild-type (wt) mice injected subcutaneously with T1525 cells and treated daily with either cromolyn or saline from day 5 after injection. One representative of 3 independent experiments (7 mice/group) is shown. B, tumor take of $Kit^{+/+}$ (wt) and $Kit^{W\text{-}sh}$ mice injected subcutaneously with T1525 cells or (C) T23 cells. Pools of 2 independent experiments (7–10 mice/group) are shown. D, tumor size (± SEM) in wt and $Kit^{W\text{-}sh}$ mice with intraprostatic injection of T1525 cells and evaluated echographically (7 mice/group). E, echographic imaging of the only tumor grown in $Kit^{W\text{-}sh}$ mice of 7 injected orthotopically in comparison with 1 representative tumor grown in wt mice (100% tumor take). White lines outline tumor mass. *, $P < 0.05$; **, $P < 0.01$; ***, $P < 0.005$. *ns*, not significant.

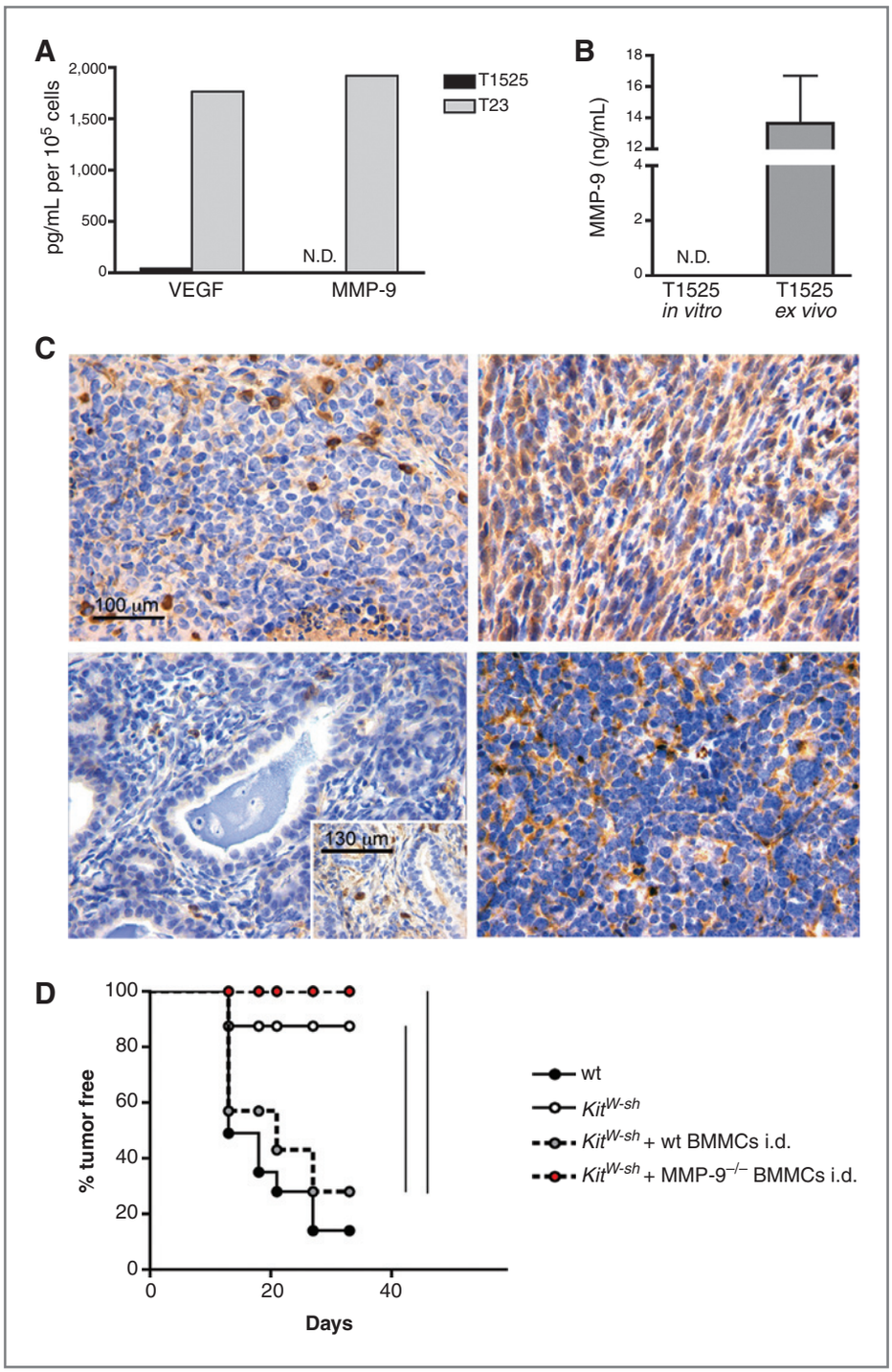

Figure 4. MCs promote WD prostate tumor growth through MMP-9 production. A, concentration of VEGF and MMP-9 secreted by T1525 and T23 cells *in vitro* measured by ELISA after 48 hours of culture. N.D., not detectable. B, concentration of MMP-9 secreted by T1525 cells *in vitro* and by T1525 tumor tissue cultured *ex vivo*. C, IHC for MMP-9 of tumors originated by subcutaneous injection of T1525 (top left) and T23 (top right) cells in wild-type (wt) mice; WD (bottom left) and PD (bottom right) foci from TRAMP tumors. D, tumor take of T1525 line injected subcutaneously in wt, $Kit^{W\text{-}sh}$, and $Kit^{W\text{-}sh}$ mice reconstituted intradermally with wt or MMP-$9^{-/-}$ BMMCs. One representative of 2 independent experiments (7 mice/group) is shown. **, $P < 0.01$.

to neoangiogenesis. Notably, the mature form of MMP-9 localizes within the secretory granules of MCs (30); therefore, its secretion is inhibited by cromolyn treatment. We hypothesized that, upon progression and EMT, prostate tumors become MC-independent, thanks to a newly acquired ability to produce protumoral factors. We therefore interrogated gene expression profiles of WD and PD tumor cell lines to identify genes encoding factors involved in angiogenesis and invasion and found that *Vegf* and *Mmp9* were upregulated in PD compared with WD tumors (3- and 2.44-fold, respectively), a finding confirmed at the protein level by assessing VEGF and MMP-9 molecules in culture supernatants (Fig. 4A). The inability to produce MMP-9 by WD line T1525 *in vitro* prompted us to verify whether

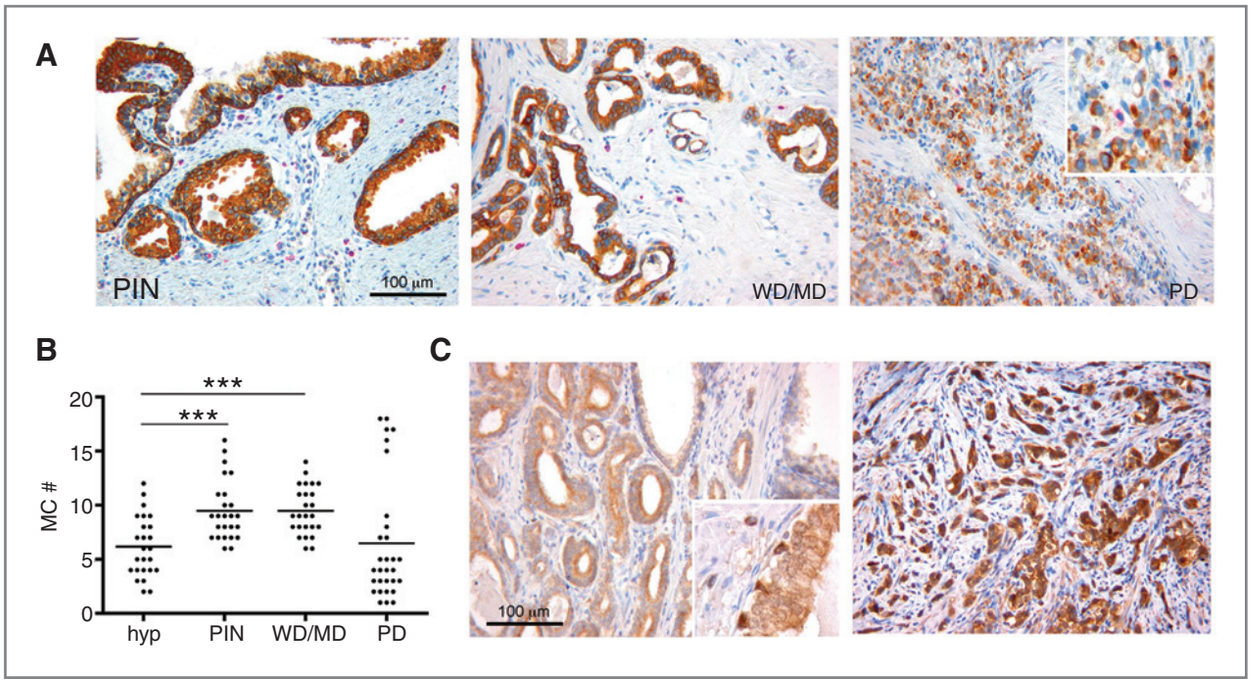

Figure 5. Human prostate carcinoma samples display the same pattern of MC infiltration and MMP-9 expression of TRAMP tumors. A, IHC double staining for MC tryptase (purple signal) and cytokeratin (brown signal) of representative samples of human biopsies characterized by atypical epithelial hyperplasia/PIN, WD or moderately differentiated (MD) adenocarcinoma, and PD adenocarcinoma. B, MC counts carried out on tryptase-stained sections from 5 WD (Gleason score 2–3) and 6 PD (Gleason score 9–10) cases classified according to histologic type. hyp, epithelial hyperplasia. C, IHC staining for MMP-9 of representative samples of human WD adenocarcinoma (left) and PD adenocarcinoma (right).

this factor is provided by tumor-infiltrating stromal cells *in vivo*. Culture supernatants of excised WD T1525 tumor tissue *ex vivo* contained very high levels of MMP-9 (Fig. 4B). Immunohistochemistry (IHC) analysis confirmed that MMP-9 was diffusely expressed by T23 neoplastic cells whereas it was absent in T1525 neoplasms. Rather, in T1525 tumors, MMP-9 was focally expressed by scattered cells, whose morphology and distribution were consistent with that of infiltrating MCs (Fig. 4C, top). This feature was reproduced in TRAMP mice (Fig. 4C, bottom), where scattered MCs accounted for MMP-9–expressing cells in WD cancer foci whereas cancer cells expressing directly MMP-9 were only found in PD foci.

In vitro, invasiveness through a basement membrane required MMP-9; accordingly, PD T23 cells were invasive whereas T1525 cells were not, unless in the presence of supernatant from activated wild-type, but not MMP-9$^{-/-}$, BMMCs (Supplementary Fig. S5B). To confirm, *in vivo*, that the role of MCs in promoting WD prostate tumor growth relied on their MMP-9 production, we derived BMMCs from MMP-9$^{-/-}$ mice to reconstitute *Kit*$^{W\text{-}sh}$ mice. Although purity and dermal reconstitution efficiency of BMMCs were equal for MMP-9$^{-/-}$ and wild-type BMMCs (not shown), the injection of T1525 cells produced tumors only in *Kit*$^{W\text{-}sh}$ mice reconstituted with wild-type, but not with MMP-9$^{-/-}$, BMMCs (Fig. 4D).

Collectively, these results indicate that MCs support WD prostate tumors by producing MMP-9.

Human prostate carcinoma samples display the same pattern of MC infiltration and MMP-9 expression of TRAMP tumors

To explore whether MCs producing MMP-9 might also associate with adenocarcinomas arising in human prostate, 5 WD (Gleason score 2–3) and 6 PD (Gleason score 9–10) prostate cancers were investigated for the amount and distribution of tryptase-positive MCs and MMP-9 expression by IHC. Notably, neoplastic foci from WD cancers were populated by a relevant amount of tryptase-positive cells, found in close contact with cytokeratin-stained cancer cells. PD cancers, conversely, showed only very few scattered tryptase-positive MCs infiltrating the neoplastic foci (Fig. 5A and B). Coherently with the dynamics observed in mice, MMP-9 expression proved to be almost entirely confined to MCs in WD human prostate cancers whereas it was found in the neoplastic cells of PD ones (Fig. 5C). Altogether, these data support the extension of the proposed role of MCs in fostering the development and progression of mouse prostate adenocarcinomas to the human pathologic setting.

MC targeting in TRAMP mice gives rise to aggressive NE tumors expressing c-Kit

The aforementioned data suggested to test whether MC targeting could hamper prostate tumorigenesis in the TRAMP model. Cromolyn (10 mg/kg i.p.) was given to TRAMP mice daily, starting from 6 to 8 weeks of age until 24 weeks of age, and tumor growth was monitored using

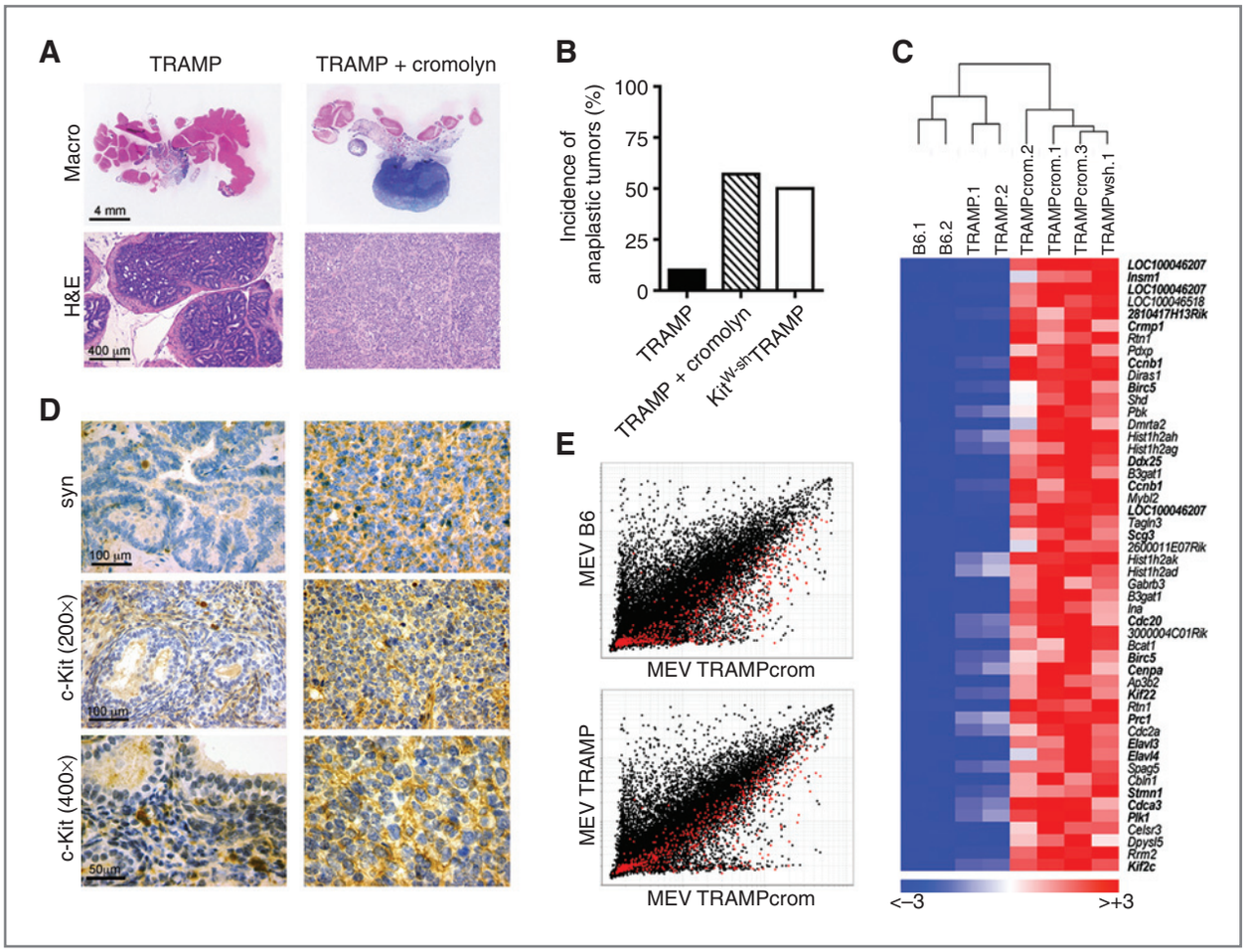

Figure 6. MC targeting in TRAMP mice gives rise to aggressive c-Kit–expressing NE tumors. A, representative macroscopic appearance (macro; top) and hematoxylin and eosin (H&E) staining (bottom) of tumors developed in TRAMP and in cromolyn-treated TRAMP mice. B, incidence of anaplastic tumors (calculated as the number of mice developing anaplastic tumors/total mice) arising in TRAMP, cromolyn-treated TRAMP, and $Kit^{W\text{-}sh}$TRAMP mice (>10 mice/group). C, hierarchical clustering of the top 50 probes upregulated in prostates from 24 weeks old TRAMP treated with cromolyn and $Kit^{W\text{-}sh}$TRAMP mice compared with 30 weeks old wild-type (B6) and TRAMP prostates. Red and blue indicate relative expression superior or inferior to the gene-wise mean, as indicated in the legend. Probes in bold are part of the published NE signature (31). D, representative IHC staining for synaptophysin (syn) and c-Kit of tumors developing in TRAMP and in cromolyn-treated TRAMP mice. E, mean expression value (MEV) plots of genes expressed by cromolyn-treated TRAMP tumors versus wild-type prostates (top) or versus TRAMP tumors (bottom). Each dot represents a probe of the 25,697 analyzed. Red dots indicate probes that are part of the published NE signature.

noninvasive 3-dimensional ultrasound imaging technology as previously described (16). Strikingly, in TRAMP mice chronically treated with cromolyn, fast growing isoechoic prostatic tumors originating in the ventral lobe were detectable in approximately 50% of mice already at 18 weeks of age and mice had to be sacrificed at 24 weeks of age because of excessive tumor burden. The remaining 50% had no detectable tumor masses by ultrasound imaging carried out at 18 and 24 weeks of age. Histologically, the rapidly growing tumors were characterized by sheets of highly anaplastic cells (Fig. 6A) whereas the prostates without tumor at echographic inspection showed, at worst, signs of glandular epithelial hyperplasia and/or foci of locally infiltrating adenocarcinoma (not shown). Similarly, early anaplastic tumors arose from the ventral prostate in 50% of $Kit^{W\text{-}sh}$TRAMP double mutants. This increased occurrence of early anaplastic tumors was clearly associated with MC inactivation/depletion, in view of an overall incidence of similar tumors in less than 10% of all TRAMP mice in our colony (Fig. 6B). Gene expression profiles of these tumors compared both with TRAMP adenocarcinomas and with normal prostates excluded early EMT while underscored a marked NE differentiation (Fig. 6C). Genes upregulated in tumors from cromolyn-treated TRAMP mice were significantly enriched for genes (listed in bold) belonging to a published "NE prostate tumor molecular signature," obtained by integration of expression profiles of NE tumors from Cr2-TAg mice (31) and human patients (ref. 32; indicated by red dots in Fig. 6E). Accordingly, tumors from cromolyn-treated TRAMP (Fig. 6D, top) and $Kit^{W\text{-}sh}$TRAMP

mice (not shown) showed extensive and uniform expression of the neuronal marker synaptophysin.

In view of the stem cell origin hypothesis of NE tumors in TRAMP mice (33, 34) and of c-Kit expression by prostate stem cells (35), we tested whether the tumors from cromolyn-treated TRAMP and $Kit^{W\text{-}sh}$TRAMP mice expressed the c-Kit receptor (Fig. 6D, bottom); accordingly, c-Kit staining was restricted to MCs scattered in prostate adenocarcinomas in TRAMP mice whereas diffused and homogenously expressed at significant levels by tumor cells in cromolyn-treated TRAMP mice (Fig. 6D, bottom). Also, tumoral c-Kit was detected in $Kit^{W\text{-}sh}$TRAMP mice (Supplementary Fig. S6), indicating that the $Kit^{W\text{-}sh}$ mutation does not affect c-Kit expression by prostate cells. Interestingly, *Kit* gene was part of the published NE molecular signature, indicating it as a common trait of prostate NE tumors.

Together, these results show that MC functional inactivation or genetic ablation in TRAMP mice results in high incidence of early-onset c-Kit$^+$ NE tumors.

Discussion

The study of the role of MCs in prostate tumorigenesis is complicated by the multifocality of prostate cancer, in which several tumor foci with different molecular and proliferative characteristics may originate and coevolve within the same organ. We have found that MCs infiltrating prostate tumors in TRAMP mice and humans increase in number upon disease progression. This and other findings (12, 36) would indicate that the inhibition of MC functions could be a new treatment of early-stage prostate cancer. However, our fine analysis of the complex relations existing between MCs and prostate tumors indicates an actual risk for more aggressive tumors in case MCs are depleted/inactivated.

We established new tumor cell lines phenocopying the different histologic and functional features of TRAMP tumors and showed that MCs promote tumor growth of WD adenocarcinoma by providing MMP-9. This finding fostered the idea of MC targeting as a way to impair tumor growth, which is also in line with a study carried out in rats showing that peritumoral MCs stimulate prostate tumor growth by providing proangiogenic factors (14).

MMP-9–producing cells of bone marrow origin have been shown to promote skin squamous carcinogenesis (37). MMP-9 has been indicated to correlate with progression of prostate tumor in humans (38) while excluded to have a role in the induction of NE tumors in the Cr2-TAg mouse model (39). Degrading the ECM, MMP-9 confers a more permissive environment for cell migration and invasion and provides the enzymatic cleavage necessary for release and activation of growth factors.

In contrast, PD prostate tumors showing features of EMT produce MMP-9 autocrinously and are devoid of infiltrating MCs both in mouse and in humans. Their MC independence may imply that MC inactivation would be ineffective in the therapy for advanced tumors. Moreover, this finding points to the critical need of indicating the exact Gleason score when prognosis is correlated to MC density, otherwise discrepancies between different studies may emerge (12, 13).

When MC targeting was applied to transgenic prostate tumors, by treating TRAMP mice chronically with cromolyn (from 6–8 weeks of age, well before the earliest evidence of disease) or by crossing TRAMP mice with $Kit^{W\text{-}sh}$ mice, we paradoxically increased the occurrence of aggressive prostate tumors, identifiable already at 18 weeks of age. These tumors displayed the molecular and histologic features of overt NE differentiation. NE cells are part of the normal prostate epithelium, together with luminal (secretory) and basal cells. NE and secretory cells arise both from a common progenitor, adult prostate stem cell, which persists in the adult organ, most probably confined within the basal cell compartment (35, 40). In the TRAMP model, SV40 TAg initiates transformation not only in luminal cells but also in prostate stem cells, because both components are androgen responsive. Current models of prostatic tumorigenesis propose that, whereas epithelial tumors are derived from the proliferation of transformed luminal cells, NE carcinomas arise independently by the NE transdifferentiation of transformed prostate stem cells (33, 34). These indications suggest that, in MC-targeted TRAMP mice, the higher incidence of NE prostate tumors might derive from the dysregulation of prostate stem cells. A possible explanation comes from the expression of c-Kit receptor, which is common to prostate stem cells (35) and to resident MCs, scattered in the stroma surrounding prostatic glands. Both cell types are dependent on the availability of the common SCF ligand to function correctly; MCs require SCF for survival and functional activation, whereas prostate stem cells apparently require c-Kit signaling for prostate regeneration (35). It is tempting to speculate that a previously unrecognized MC role may be the maintenance of prostate stem cell homeostasis by keeping local SCF availability in check; MCs may control NE tumor formation, serving as "natural decoys" that sequester SCF, thus limiting c-Kit signaling in TAg-transformed prostate stem cells. According to this hypothesis, c-Kit$^+$ NE tumors would be more likely to develop in the absence of MCs, or upon cromolyn treatment, which some groups have reported to hamper MC migration in response to nonhomeostatic stimuli (41). The concept of compensatory mechanisms existing between c-Kit–dependent cellular populations is corroborated by our data showing that MC reconstitution normalizes the enhanced granulocytosis characterizing $Kit^{W\text{-}sh}$ mice (17). Our hypothesis is also supported by recent results showing competition between prostate cancer cells and hematopoietic stem cells for the endosteal niche in the bone marrow (42); intriguingly, cancer cells were more competitive when expressing "stem-like" features, suggesting a potential competition for SCF, as both cancer and hematopoietic stem cells are expectedly c-Kit$^+$.

The novel role of MCs in protecting against the development of "stem-like" tumors might find correlation in humans, where NE differentiation occurs in 10% to 30% of prostate cancers, especially after hormone ablation and where tumoral c-Kit expression has been identified in a sizeable fraction of high-risk human prostate tumors (43). A similar mechanism of tumor control by MCs may be envisaged also for other nonmutated c-Kit–expressing tumors, such as Merkel carcinoma (44).

Taken together, our data underscore the crucial role of MCs in prostate tumorigenesis and show that MCs exert different functions according to tumor stage; MCs favor initial tumor growth providing MMP-9 but become dispensable after EMT. We also uncover a new role for MCs in suppressing the occurrence of c-Kit$^+$ NE tumors and point to a detrimental effect of mere MC inhibition. In this view, c-Kit tyrosine kinase inhibitors, such as imatinib, would instead offer the advantage of targeting both adenocarcinoma-promoting MCs (stroma targeting) and NE tumor variants (tumor targeting; ref. 45).

Disclosure of Potential Conflicts of Interest

No potential conflicts of interest were disclosed.

Acknowledgments

We thank Claudia Chiodoni for helpful discussion, Ivano Arioli for technical assistance with mice, Loris De Cecco for microarray data generation, and Carla Guarnotta for IHC.

Grant Support

This work was supported by grants from Fondazione Italo Monzino, the Italian Ministry of Health and Associazione Italiana Ricerca sul Cancro (to M.P. Colombo). S. Piconese is supported by My First AIRC grant (#8726). P. Pittoni is supported by a fellowship from FIRC (Fondazione Italiana Ricerca sul Cancro).

The costs of publication of this article were defrayed in part by the payment of page charges. This article must therefore be hereby marked *advertisement* in accordance with 18 U.S.C. Section 1734 solely to indicate this fact.

Received May 12, 2011; revised June 21, 2011; accepted July 20, 2011; published OnlineFirst September 6, 2011.

References

1. Jemal A, Siegel R, Xu J, Ward E. Cancer statistics, 2010. CA Cancer J Clin 2010;60:277–300.
2. Ruijter ET, van de Kaa CA, Schalken JA, Debruyne FM, Ruiter DJ. Histological grade heterogeneity in multifocal prostate cancer. Biological and clinical implications. J Pathol 1996;180: 295–9.
3. Komiya A, Suzuki H, Imamoto T, Kamiya N, Nihei N, Naya Y, et al. Neuroendocrine differentiation in the progression of prostate cancer. Int J Urol 2009;16:37–44.
4. Greenberg NM, DeMayo F, Finegold MJ, Medina D, Tilley WD, Aspinall JO, et al. Prostate cancer in a transgenic mouse. Proc Natl Acad Sci U S A 1995;92:3439–43.
5. Hurwitz AA, Foster BA, Allison JP, Greenberg NM, Kwon ED. The TRAMP mouse as a model for prostate cancer. Curr Protoc Immunol 2001;Chapter 20:Unit 20.5.
6. Tang Y, Wang L, Goloubeva O, Khan MA, Lee D, Hussain A. The relationship of neuroendocrine carcinomas to anti-tumor therapies in TRAMP mice. Prostate 2009;69:1763–73.
7. Theoharides TC, Conti P. Mast cells: the Jekyll and Hyde of tumor growth. Trends Immunol 2004;25:235–41.
8. Maltby S, Khazaie K, McNagny KM. Mast cells in tumor growth: angiogenesis, tissue remodelling and immune-modulation. Biochim Biophys Acta 2009;1796:19–26.
9. Sari A, Serel TA, Candir O, Ozturk A, Kosar A. Mast cell variations in tumour tissue and with histopathological grading in specimens of prostatic adenocarcinoma. BJU Int 1999;84:851–3.
10. Simak R, Capodieci P, Cohen DW, Fair WR, Scher H, Melamed J, et al. Expression of c-kit and kit-ligand in benign and malignant prostatic tissues. Histol Histopathol 2000;15:365–74.
11. Aydin O, Dusmez D, Cinel L, Doruk E, Kanik A. Immunohistological analysis of mast cell numbers in the intratumoral and peritumoral regions of prostate carcinoma compared to benign prostatic hyperplasia. Pathol Res Pract 2002;198:267–71.
12. Nonomura N, Takayama H, Nishimura K, Oka D, Nakai Y, Shiba M, et al. Decreased number of mast cells infiltrating into needle biopsy specimens leads to a better prognosis of prostate cancer. Br J Cancer 2007;97:952–6.
13. Fleischmann A, Schlomm T, Kollermann J, Sekulic N, Huland H, Mirlacher M, et al. Immunological microenvironment in prostate cancer: high mast cell densities are associated with favorable tumor characteristics and good prognosis. Prostate 2009;69: 976–81.
14. Johansson A, Rudolfsson S, Hammarsten P, Halin S, Pietras K, Jones J, et al. Mast cells are novel independent prognostic markers in prostate cancer and represent a target for therapy. Am J Pathol 2010;177:1031–41.
15. Foster BA, Gingrich JR, Kwon ED, Madias C, Greenberg NM. Characterization of prostatic epithelial cell lines derived from transgenic adenocarcinoma of the mouse prostate (TRAMP) model. Cancer Res 1997;57:3325–30.
16. Wirtzfeld LA, Wu G, Bygrave M, Yamasaki Y, Sakai H, Moussa M, et al. A new three-dimensional ultrasound microimaging technology for preclinical studies using a transgenic prostate cancer mouse model. Cancer Res 2005;65:6337–45.
17. Piconese S, Costanza M, Musio S, Tripodo C, Poliani PL, Gri G, et al. Exacerbated experimental autoimmune encephalomyelitis in mast-cell-deficient Kit(W-sh/W-sh) mice. Lab Invest 2011;91: 627–41.
18. Melani C, Sangaletti S, Barazzetta FM, Werb Z, Colombo MP. Amino-biphosphonate-mediated MMP-9 inhibition breaks the tumor-bone marrow axis responsible for myeloid-derived suppressor cell expansion and macrophage infiltration in tumor stroma. Cancer Res 2007;67:11438–46.
19. Gri G, Piconese S, Frossi B, Manfroi V, Merluzzi S, Tripodo C, et al. CD4$^+$CD25$^+$ regulatory T cells suppress mast cell degranulation and allergic responses through OX40-OX40L interaction. Immunity 2008;29:771–81.
20. Chirgwin JM, Przybyla AE, MacDonald RJ, Rutter WJ. Isolation of biologically active ribonucleic acid from sources enriched in ribonuclease. Biochemistry 1979;18:5294–9.
21. Reich M, Liefeld T, Gould J, Lerner J, Tamayo P, Mesirov JP. GenePattern 2.0. Nat Genet 2006;38:500–1.
22. Shappell SB, Thomas GV, Roberts RL, Herbert R, Ittmann MM, Rubin MA, et al. Prostate pathology of genetically engineered mice: definitions and classification. The consensus report from the Bar Harbor meeting of the Mouse Models of Human Cancer Consortium Prostate Pathology Committee. Cancer Res 2004; 64:2270–305.
23. Coussens LM, Raymond WW, Bergers G, Laig-Webster M, Behrendtsen O, Werb Z, et al. Inflammatory mast cells up-regulate angiogenesis during squamous epithelial carcinogenesis. Genes Dev 1999; 13:1382–97.
24. Soucek L, Lawlor ER, Soto D, Shchors K, Swigart LB, Evan GI. Mast cells are required for angiogenesis and macroscopic expansion of Myc-induced pancreatic islet tumors. Nat Med 2007;13:1211–8.
25. Thompson PJ, Hanson JM, Morley J. Asthma, mast cells, and sodium cromoglycate. Lancet 1983;2:848–9.
26. Grimbaldeston MA, Chen CC, Piliponsky AM, Tsai M, Tam SY, Galli SJ. Mast cell-deficient W-sash c-kit mutant Kit W-sh/W-sh mice as a model for investigating mast cell biology *in vivo*. Am J Pathol 2005;167:835–48.
27. Nigrovic PA, Gray DH, Jones T, Hallgren J, Kuo FC, Chaletzky B, et al. Genetic inversion in mast cell-deficient (W(sh)) mice interrupts corin and manifests as hematopoietic and cardiac aberrancy. American J Pathol 2008;173:1693–701.
28. Norrby K. Mast cells and angiogenesis. APMIS 2002;110:355–71.

29. Kanbe N, Tanaka A, Kanbe M, Itakura A, Kurosawa M, Matsuda H. Human mast cells produce matrix metalloproteinase 9. Eur J Immunol 1999;29:2645–9.
30. Baram D, Vaday GG, Salamon P, Drucker I, Hershkoviz R, Mekori YA. Human mast cells release metalloproteinase-9 on contact with activated T cells: juxtacrine regulation by TNF-alpha. J Immunol 2001; 167:4008–16.
31. Hu Y, Ippolito JE, Garabedian EM, Humphrey PA, Gordon JI. Molecular characterization of a metastatic neuroendocrine cell cancer arising in the prostates of transgenic mice. J Biol Chem 2002;277: 44462–74.
32. Ippolito JE, Xu J, Jain S, Moulder K, Mennerick S, Crowley JR, et al. An integrated functional genomics and metabolomics approach for defining poor prognosis in human neuroendocrine cancers. Proc Natl Acad Sci U S A 2005;102:9901–6.
33. Chiaverotti T, Couto SS, Donjacour A, Mao JH, Nagase H Cardiff RD, et al. Dissociation of epithelial and neuroendocrine carcinoma lineages in the transgenic adenocarcinoma of mouse prostate model of prostate cancer. Am J Pathol 2008;172: 236–46.
34. Huss WJ, Gray DR, Tavakoli K, Marmillion ME, Durham LE, Johnson MA, et al. Origin of androgen-insensitive poorly differentiated tumors in the transgenic adenocarcinoma of mouse prostate model. Neoplasia 2007;9:938–50.
35. Leong KG, Wang BE, Johnson L, Gao WQ. Generation of a prostate from a single adult stem cell. Nature 2008;456: 804–8.
36. Groot Kormelink T, Abudukelimu A, Redegeld FA. Mast cells as target in cancer therapy. Curr Pharma Design 2009;15: 1868–78.
37. Coussens LM, Tinkle CL, Hanahan D, Werb Z. MMP-9 supplied by bone marrow-derived cells contributes to skin carcinogenesis. Cell 2000;103:481–90.
38. Castellano G, Malaponte G, Mazzarino MC, Figini M, Marchese F, Gangemi P, et al. Activation of the osteopontin/matrix metalloproteinase-9 pathway correlates with prostate cancer progression. Clin Cancer Res 2008;14:7470–80.
39. Littlepage LE, Sternlicht MD, Rougier N, Phillips J, Gallo E, Yu Y, et al. Matrix metalloproteinases contribute distinct roles in neuroendocrine prostate carcinogenesis, metastasis, and angiogenesis progression. Cancer Res 2010;70:2224–34.
40. Goldstein AS, Stoyanova T, Witte ON. Primitive origins of prostate cancer: *in vivo* evidence for prostate-regenerating cells and prostate cancer-initiating cells. Mol Oncol 2010;4:385–96.
41. Jin Y, Silverman AJ, Vannucci SJ. Mast cell stabilization limits hypoxic-ischemic brain damage in the immature rat. Dev Neurosci 2007;29:373–84.
42. Shiozawa Y, Pedersen EA, Havens AM, Jung Y, Mishra A, Joseph J, et al. Human prostate cancer metastases target the hematopoietic stem cell niche to establish footholds in mouse bone marrow. J Clin Invest 2011;121:1298–312.
43. Di Lorenzo G, Autorino R, D'Armiento FP, Mignogna C, De Laurentiis M, De Sio M, et al. Expression of proto-oncogene c-kit in high risk prostate cancer. Eur J Surg Oncol 2004;30:987–92.
44. Kostoula V, Khan K, Savage K, Stubbs M, Quaglia A, Dhillon AP, et al. Expression of c-kit (CD117) in neuroendocrine tumours—a target for therapy? Oncol Rep 2005;13:643–7.
45. Pittoni P, Piconese S, Tripodo C, Colombo MP. Tumor-intrinsic and -extrinsic roles of c-Kit: mast cells as the primary off-target of tyrosine kinase inhibitors. Oncogene 2010;30:757–69.